Journal of Zhejiang University SCIENCE A
ISSN 1673-565X (Print); ISSN 1862-1775 (Online)
www.zju.edu.cn/jzus; www.springerlink.com
E-mail: jzus@zju.edu.cn

Study on hydrodynamic vibration in fluidic flowmeter*

WANG Chi-yu, ZOU Jun†‡, FU Xin, YANG Hua-yong

(*Institute State Key Laboratory of Fluid Power Transmission and Control, Zhejiang University, Hangzhou 310027, China*)

†E-mail: junzou@zju.edu.cn

Received Mar. 10, 2007; revision accepted June 11, 2007

Abstract: The characteristics of the fluidic flowmeter, which is a combination of impinged concave wall and bistable fluid amplifier, is investigated by experimental studies and numerical simulations. The numerical approaches are utilized to examine the time dependent flow field and pressure field inside the proposed flowmeter. The effect of varying structural parameters on flow characteristics of the proposed fluidic flowmeter is investigated by computational simulations for the optimization. Both the simulation and experimental results disclose that the hydrodynamic vibration, with the same intensity, frequency and 180° phase shift, occurs at axisymmetric points in the feedback channel of the fluidic flowmeter. Using the structural combination of impinged concave wall and bistable fluid amplifier and differential signal processing technique, a novel fluidic flowmeter with excellent immunity and improved sensibility is developed.

Key words: Flowmeter, Fluidic, Hydrodynamic vibration, Coanda effect
doi:10.1631/jzus.2007.A1422 **Document code:** A **CLC number:** TH137

INTRODUCTION

A stream of fluid emerging from a nozzle tends to follow a nearby curved surface, known as Coanda effect, if the curvature of the surface or the angle that the surface makes with the stream is not too sharp. This tendency is caused by the nearby fluid molecules entrained by the jet stream. Because the supply of these molecules is limited by an adjacent surface, a partial vacuum emerges between the jet stream and surface, while the pressure on the other side of the jet stream remains constant. The differential pressure between both sides of the jet stream will force the jet to bend and attach itself to the wall.

The fluidic flowmeter based on Coanda effect emerged in the late 1960's (Davies, 1970; Tippetts *et al*., 1973). Since there is no moving part in this flowmeter, there is little for wear or physical damage caused by foreign matter (Boucher and Mazharoglu, 1988). In addition, it has many attractive advantages, for instance, high reliability, low cost, wide measurement range and insensitivity to fluid properties and temperature. It has been widely accepted that the fluidic flowmeter is a promising flow instrument for measuring gas and liquid fluids, multiphase flow, unclean fluids, high viscosity fluids and corrosive fluids in the chemical and petroleum industry, especially at low Reynolds numbers compared with other fluid oscillatory type flowmeters (Wang *et al*., 1996; Priestman and Boucher, 2005; 2006), such as vortex shedding flowmeter and vortex-precession swirlmeter.

There are two main design principles of the fluidic oscillator: the generation of self-induced and sustained oscillations of the flow that has a frequency which is proportional to the flow velocity and the invariableness of Strouhal number. Many different designs were investigated and implemented for the creation of the jet oscillation and the stability of Strouhal number. Mansy and Williams (1989) investigated a trapped vortex pair oscillator, in which a pair of vortices is trapped in a convergent elliptical

‡ Corresponding author
* Project supported by the National Basic Research Program (973) of China (No. 2006CB705400) and the National Natural Science Foundation of China (No. 50575200)

channel. Parry *et al*.(1991) investigated a target fluidic oscillator, in which the jet oscillation is created due to the interaction of a planar jet with a bluff body. Uzol and Camci (1998) proposed a kind of fluidic oscillator which creates a jet oscillation due to the impingement of the jet on a concave wall. Gao *et al*. (1999) and Nakayama *et al*.(2005) proposed a kind of fluidic oscillator which creates a jet oscillation based on bistable fluid amplifier, and is applied in petroleum machinery widely.

The aims of this paper were to determine the flow characteristics of a fluidic flowmeter, which is a combination of impinged concave wall and bistable fluid amplifier (Grigorievich, 2003), by experimental studies and numerical simulations. The jet oscillation inside the fluidic oscillator is investigated in detail in order to obtain more information about the physical mechanisms that drive the jet oscillation inside the oscillation chamber. The jet oscillation frequency is measured by pressure sensors. Computational simulations are performed to assess the accuracy of such a numerical technique by comparing the simulated oscillation frequency with the experimental value. The effect of varying structural parameters on the flow characteristics of the proposed fluidic flowmeter is investigated by computational simulations for the optimization. Furthermore, both the simulation and observation results disclose that the hydrodynamic vibration, with the same intensity, frequency and 180° phase shift, occurs at axisymmetric points in the feedback channel of the fluidic flowmeter.

NUMERICAL INVESTIGATION

Large eddy simulation (LES) model

The governing equations of LES (Su, 1984; Fu and Yang, 2001) are obtained by filtering the time-dependent N-S equations. A filtered variable is defined by

$$\overline{\phi}(x)=\int_{D_f}\phi(x')G(x,x')\mathrm{d}x', \tag{1}$$

where D_f is fluid domain; $G(\cdot)$ is filter function determining scale of resolved eddies.

For the finite-volume discretization, the filtering operation is provided by

$$\overline{\phi}(x)=\frac{1}{V}\int_v\phi(x')\mathrm{d}x',\ x'\in v, \tag{2}$$

where V is Volume of a computational cell, mm^3; v is computational cell domain.

The filter function implied here is then

$$G(x,x')=\begin{cases}1/V, & \text{for } x'\in v;\\ 0, & \text{otherwise.}\end{cases} \tag{3}$$

Ignoring the energy transport, the filtered N-S equations are then

$$\frac{\partial\rho}{\partial t}+\frac{\partial\rho\overline{u}_i}{\partial x_i}=0, \tag{4}$$

$$\frac{\partial}{\partial t}(\rho\overline{u}_i)+\frac{\partial}{\partial x_j}(\rho\overline{u}_i\overline{u}_j)=\frac{\partial}{\partial x_j}\left(\mu\frac{\partial\overline{u}_i}{\partial x_j}\right)-\frac{\partial\overline{p}}{\partial x_i}-\frac{\partial\tau_{ij}}{\partial x_j}, \tag{5}$$

$$\tau_{ij}=\overline{u_iu_j}-\overline{u}_i\overline{u}_j, \tag{6}$$

where ρ is fluid density, kg/m^3; μ is fluid viscosity, kg/(m·s); τ_{ij} is subgrid-scale stress.

The unknown subgrid-scale stresses can be modeled by eddy viscosity in the following form:

$$\tau_{ij}-\frac{1}{3}\tau_{kk}\delta_{ij}=-2\mu_t\overline{S}_{ij}, \tag{7}$$

$$\overline{S}_{ij}\equiv\frac{1}{2}\left(\frac{\partial\overline{u}_i}{\partial x_j}+\frac{\partial\overline{u}_j}{\partial x_i}\right), \tag{8}$$

$$\mu_t=\rho L_s^2\left|\overline{S}\right|, \tag{9}$$

$$L_s=\min(\kappa d, C_sV^{1/3}), \tag{10}$$

$$\left|\overline{S}\right|\equiv\sqrt{2\overline{S}_{ij}\overline{S}_{ij}}, \tag{11}$$

where μ_t is subgrid-scale turbulent viscosity; $\overline{S}_{ij}$ is rate-of-strain tensor for the resolved scale; L_s is mixing length for subgrid scales; κ is model constant, κ=0.42; d is control port width, mm; C_s is smagorinsky constant, C_s=0.1 (Liu *et al*., 2005).

Geometry parameters and grid generation

The proposed fluidic flowmeter is comprised of oscillation chamber, feedback channels, concave wall, etc. A jet stream flows through the chamber, and some of the fluid will impact the jet from the side because of the feedback channels. This causes a pressure differential between one side of the jet and the other, and the jet stream swings back and forth in the oscillation

chamber (Boucher, 1995). The flow recirculation paths play an important role in the performance of the flowmeter. Two of the important parameters (Parry *et al*., 1991) to generate and provide the recirculation path are the width of the jet b and the distance l between jet nozzle and concave wall as shown in Fig.1. The five observation points are defined in the feedback channels. The locations of point 3 and point 5 are symmetric. If the flow rate is too low, flow oscillation will not occur. The flow oscillation starts when the Reynolds number exceeds the minimum of flowmeter. The parameters mentioned above will affect the relationship of Strouhal number and Reynolds number, and the quality of the oscillation signal.

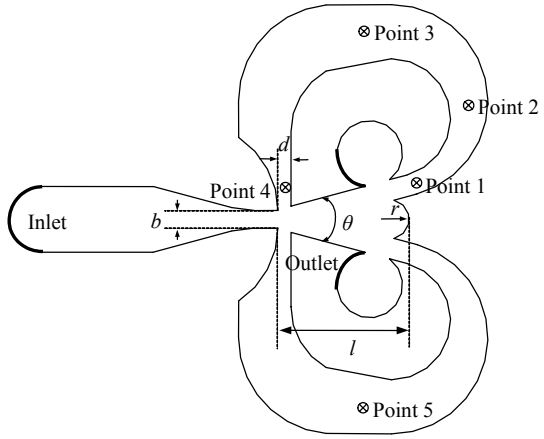

Fig.1 Structural parameters of fluidic flowmeter (θ is angle of wall, r is Radius of concave wall)

The geometry of the flowmeter has been meshed by an advanced grid preprocessor, Gambit 2.0, using triangle three-node elements and unstructured grids in order to follow as close as possible the structure of the flowmeter. For better resolution of the features of the flow field, the solution-adaptive grid feature of Fluent 6.0 is applied to refine the original mesh based on the geometry, boundary and numerical values of velocity gradient and pressure gradient. The adapted final grid is presented in Fig.2. The total number of nodes used for simulation analysis of it is approximately 10^4, the maximum grid density is 1.17×10^4 mm^{-2}, and the minimum is 7.13×10^2 mm^{-2}.

Simulation conditions

The fluid dynamic performance within the fluidic flowmeter has been computed by the commercial software Fluent 6.0 under various ratios of b/l. The

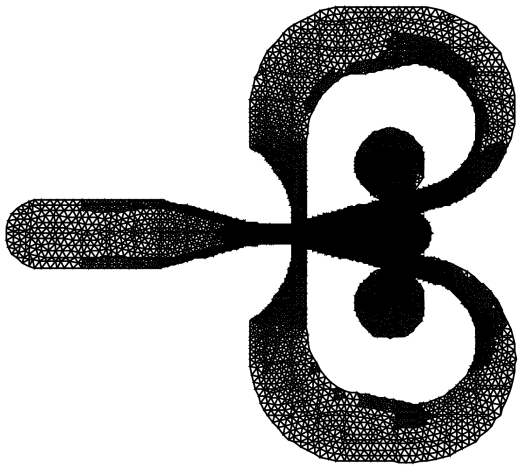

Fig.2 Grid of the fluid domain

other simulation conditions are specified as follows:

(1) The boundary conditions are specified at the velocity inlet and pressure outlet with the various inlet velocity of U_{in}=1~40 m/s (Re=684.6~27384) and the constant pressure outlet of P_{out}=0 Pa. As the energy equation is neglected in the simulation model, no heat transfer between the fluid zone and the solid zone is considered.

(2) The initial conditions are assumed as u_i=0 and p_i=0 at all the nodes in the calculational fluid domain. The fluid to be simulated is air with properties of ρ=1.225 kg/m^3, μ=1.7894×10^{-5} kg/(m·s).

(3) In the time-dependent computation procedure, the first-order implicit formulation is specified. For the discretization treatment, the PISO (Pressure Implicit Solution by Split Operator) algorithm is selected as the pressure-velocity coupling, and the second-order for the pressure and second-order upwind for the momentum are defined. In order to model transient phenomena properly, the time step size (Δt) is set about one twentieth of fluidic swing period (T_v), thus, $\Delta t=T_v/20$.

(4) The convergence criteria used to terminate the iterative process of solution are based on the control of both the solution and the residual vector. The under-relaxation factors, which are used for pressure, mass, density and body force respectively, for controlling convergence of iteration process are specified, at k_p=0.25, k_m=0.7, k_d=1 and k_b=1. The convergence control is based on the evaluation of the relative deviation, and every solution is accepted when the tolerance of each variable becomes lower than 10^{-4}.

EXPERIMENTAL SETUP

The schematic diagram of the experimental setup is shown in Fig.3. The measuring transducers are two piezoelectric pressure sensors, which are stuck on the feedback channel wall at the position of point 3 and point 5 respectively as shown in Fig.1. The sensor signals are amplified by the input amplifier, and then transmitted to the computer through data acquisition card (NI-6071E). The data processing and analyzing are carried out by the commercial software package (Labview 7.0). The mass flowrate in the experimental system is controlled by flow regulating valve and read out by a roots flowmeter (B3-7M175). The fluidic flowmeter tested in the experiment is with the same dimension as in the simulation. The structural parameters of the fluidic flowmeter used in the experiment are listed in Table 1. The fluid used in the experiment is air flowing at Reynolds number (*Re*) between 684.6 and 27384.

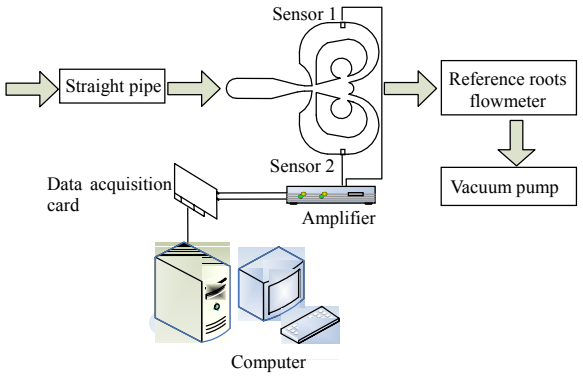

Fig.3 Schematic diagram of experimental setup

Table 1 Structural parameters of the fluidic flowmeter in the experiment

Structural parameters	Value
b (mm)	4
d (mm)	6
l (mm)	30
r (mm)	4.5
θ (°)	30

RESULTS AND DISCUSSION

Fig.4 illustrates a set of typical instant velocity fields in the fluidic flowmeter from the time dependent simulation at a Reynolds number of 3542. It can be seen that the jet oscillation occurs inside the fluidic oscillation chamber because the Coanda effect works. The jet stream, swinging back and forth in the oscillation chamber, induces periodical pressure oscillation as shown in Fig.5. The computed frequency is 62.5 Hz while the experimental frequency for the same Reynolds number of 3542 is 59.7 Hz, giving a deviation of 4.6%. But the simulation results, based on the 2D model of the fluidic flowmeter, are only indicative.

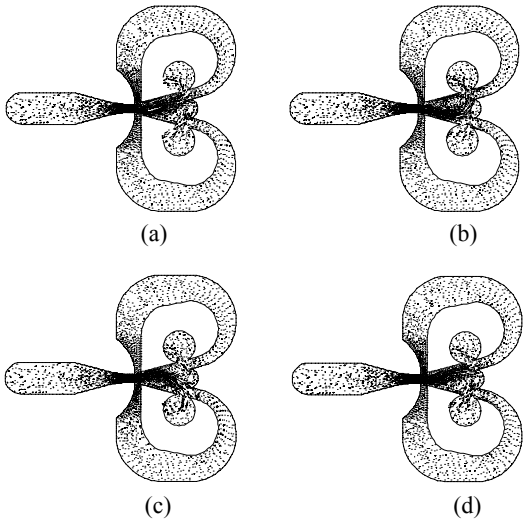

Fig.4 Velocity fields of fluidic flowmeter. (a) Time=502 ms; (b) Time=508 ms; (c) Time=514 ms; (d) Time=520 ms

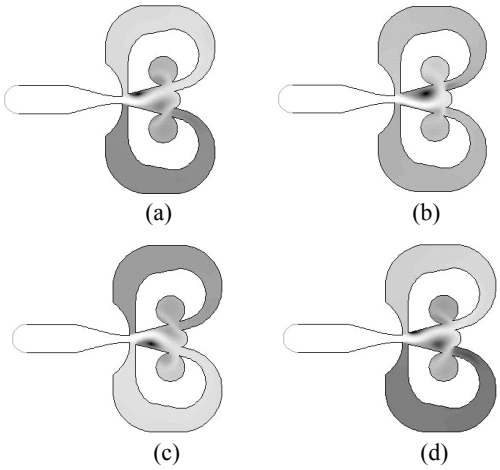

Fig.5 Pressure fields of fluidic flowmeter. (a) Time=502 ms; (b) Time=508 ms; (c) Time=514 ms; (d) Time=520 ms

Fig.6 compares the simulated hydrodynamic vibrations at the five observing points shown in Fig.1. It can be seen that the vibration frequency at the five points in feedback channel is the same. The vibration

amplitude at point 1, which is close to the entrance of feedback channel, is the largest. However, it is almost the same at other observing points. At the axisymmetric points of the fluidic flowmeter, point 3 and point 5, the hydrodynamic vibrations have a phase shift of 180°.

Figs.7~9 present the simulation results that illustrate the effects of the varying structural parameters on the vibration intensity, the Strouhal number (*St*) and the pressure loss of the proposed fluidic flowmeter. From these figures, it can be seen that the ratio of *l*/*b*, the distance between jet nozzle and concave wall versus the width of jet, affects the vibration intensity, Strouhal number and pressure lost. As the ratio *l*/*b* increases, the vibration intensity and pressure lost increase, while the Strouhal number decreases.

Fig.10 shows the measurement results of the pressure signal at point 3 and point 5 in the feedback channel of the fluidic flowmeter. It can be seen that the signals from two sensors have almost the same intensity and frequency but 180° phase shift. The differential signal of two sensors has the same frequency and double intensity. It has a very important advantage of suppressing the common mode noise from environmental disturbance.

The Strouhal number is a function of frequency, characteristic length and flow velocity. In a fluidic flowmeter, it is defined by (Fu *et al*., 2005)

$$St = fD/U, \tag{12}$$

$$St = F\left(\frac{\zeta}{2}, \frac{b}{l}, \frac{d}{l}, \frac{r}{l}, Re\right). \tag{13}$$

When the structural parameters of the fluidic flowmeter are determined, the Strouhal number only varies with Reynold number. The relationship of Strouhal number versus Reynolds number is shown in Fig.11. When the inlet Reynolds number is less than 2000, or is more than 20000, the deviation of Strouhal number is relatively large. This is due to the nonlinear characteristics of the flowmeter (Boucher and Mazharoglu, 1988; Boucher *et al*., 1996).

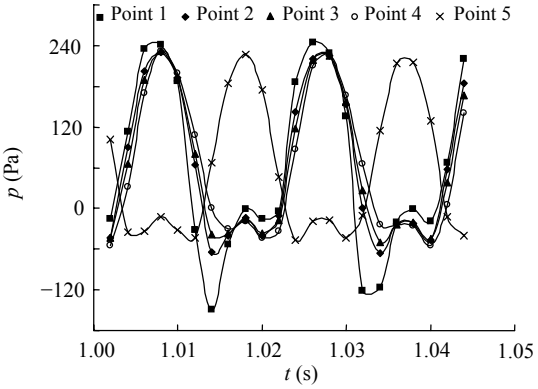

Fig.6 Pressure at different point in the fluidic flowmeter (U_{in}=5.04 m/s, p_{out}=0 Pa, *Re*=3542, Δ*t*=1 ms, *l*/*b*=7.5)

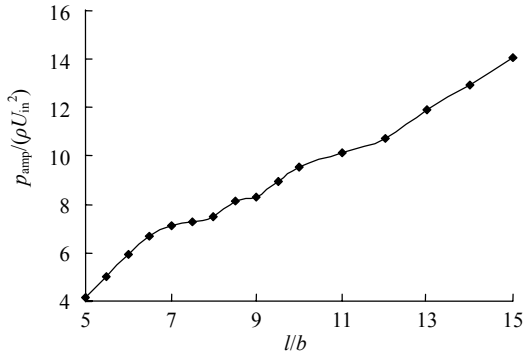

Fig.7 Effects of the structural parameters *l*/*b* on vibration intensity (U_{in}=5.04 m/s, p_{out}=0 Pa, *Re*=3542, Δ*t*=1 ms, *l*/*b*=5~15, point 3)

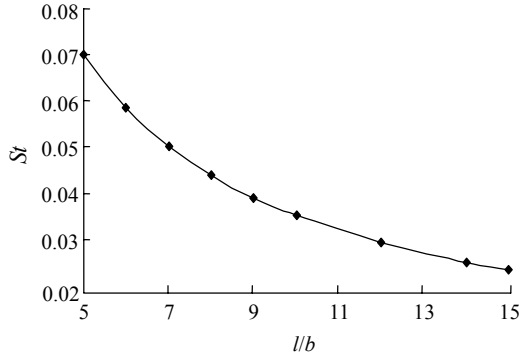

Fig.8 Effects of the structural parameters *l*/*b* on Strouhal number (U_{in}=5.04 m/s, p_{out}=0 Pa, *Re*=3542, Δ*t*=1 ms, *l*/*b*=5~15, point 3)

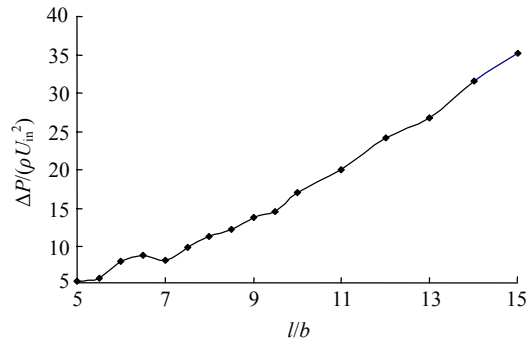

Fig.9 Effects of the structural parameters *l*/*b* on pressure loss (U_{in}=5.04 m/s, p_{out}=0 Pa, *Re*=3542, Δ*t*=1 ms, *l*/*b*=5~15, point 3)

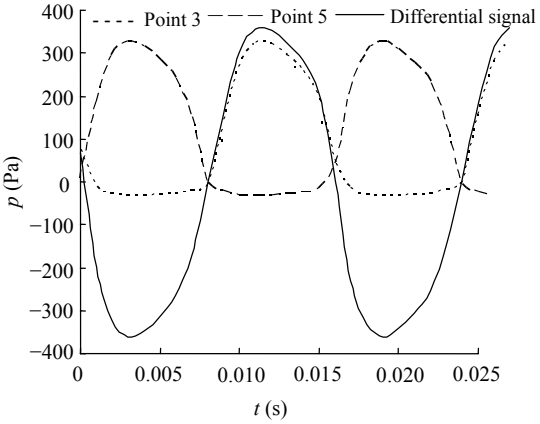

Fig.10 Experimental results of hydrodynamic vibration (U_{in}=5.09 m/s)

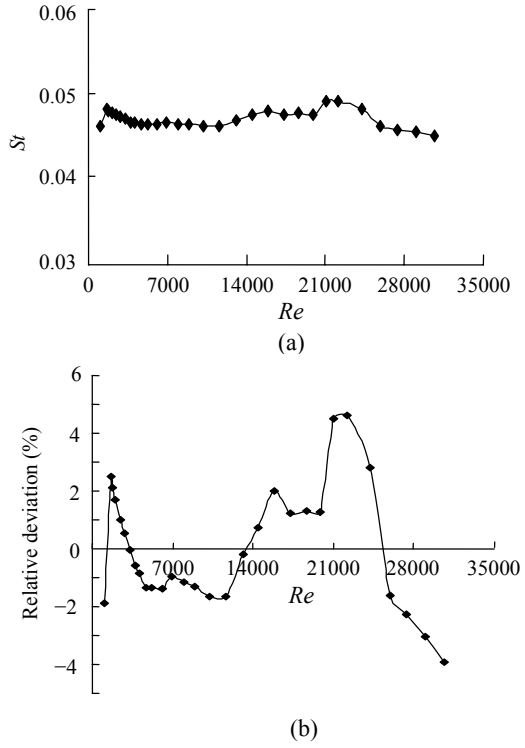

Fig.11 Relationship of the Strouhal number versus Reynolds number in experiment. (a) Experimental data of the Strouhal number; (b) Relative deviation of the Stouhal number

CONCLUSION

The objective of this work is to improve the sensibility and signal quality of fluidic flowmeter. The effect of varying structural parameters on flow characteristics of the fluidic flowmeter is investigated by computational simulations for the optimization. The ideal location for placing the piezoelectric pressure sensor in the proposed fluidic flowmeter is determined by computational fluid dynamics. This location was near to feedback channel intake. The structural combination of concave wall and fluidic amplifier can induce the fluidic vibration easily and strengthen the hydrodynamic vibration significantly. Based on simulation and experimental results, it is proved that using the differential signal of two sensors, fixed on axisymmetric points in feedback channel of the flowmeter, has a very important advantage of suppressing the common mode noise from environmental disturbance.

References

Boucher, R.F., 1995. Minimum flow optimization of fluidic flowmeters. *Measurement Science and Technology*, **6**(7): 872-879. [doi:10.1088/0957-0233/6/7/003]

Boucher, R.F., Mazharoglu, C., 1988. Low Reynolds number fluidic flowmetering. *Journal of Physics E: Scientific Instruments*, **21**(10):977-989. [doi:10.1088/0022-3735/21/10/015]

Boucher, R.F., Beck, S.B.M., Wang, H., 1996. A fluidic flowmetering device for remote measurement. *Journal Process Mechanical Engineering*, **210**(2):93-100.

Davies, R.C., 1970. Functional characteristics of fluid elements. *Fluidics Quarterly*, **2**(2):1-43.

Fu, X., Yang, H.Y., 2001. Study on hydrodynamic vibration in dual bluff body vortex flowmeter. *Chinese Journal Chemistry Engineering*, **9**(2):123-128.

Fu, X., Wang, C.Y., Xie, H.B., Yang, H.Y., 2006. Numerical simulation and experimental study on fluidic flowmeter. *Chinese Journal Mechanical Engineering*, **42**(7):24-29 (in Chinese).

Gao, J.N., Ma, J.G., Jiang, Y., Liu, C.L., 1999. Mechanism and simulation of hydraulic bistable fluidic oscillator. *China Petroleum Machinery*, **26**(6):33-35 (in Chinese)

Grigorievich, Z.E., 2003. Струйного Автогенератора. Chinese-Russian Academic Exchanges on Key Technology of Electromagnetic Flowmeter. Fluidic Flowmeter & Vortex Procession Flowmeter, Institut Teploehnergeticheskogo Pri, Moscow.

Liu, X.B., Zeng, Y.Z., Huang, H., 2005. Numerical Prediction of pressure fluctuation within francis turbine for large-eddy simulation. *Journal of Xihua University*, **24**(1):1-6 (in Chinese).

Mansy, H., Williams, D.R., 1989. An experimental and numerical study of trapped vortex pair fluidic flowmeter. *ASME FED Forum on Turbulent Flow*s, **76**:35-39.

Nakayama, A., Kuwahara, F., Kamiya, Y., 2005. A two dimensional numerical procedure for a three dimensional

internal flow through a complex passage with a small depth. *International Journal Numerical Methods for Heat & Fluid Flow*, **15**(8):863-871. [doi:10.1108/09615530510625129]

Parry, A.J., Chiwanga, S.G., Kalsi, H.S., Jepson, P., 1991. Numerical and experimental visualization of flow through a target fluidic oscillator. *ASME FED Experimental and Numerical Flow Visualization*, **128**:327-334.

Priestman, G.H., Boucher, R.F., 2005. The biased laminar by-pass fluidic flowmeter. *Journal of Fluids Engineering*, **127**(6):1199-1204. [doi:10.1115/1.2060729]

Priestman, G.H., Boucher, R.F., 2006. Smart fluidic meters for simultaneous measurement of fluid flowrate, Reynolds number, density and viscosity. *Journal of Chemical Engineering of Japan*, **39**(4):383-393. [doi:10.1252/jcej.39.383]

Su, M.D., 1984. Large eddy simulation—A new method for studying turbulence. *Advances in Mechanics*, **14**(4):440-452.

Tippetts, J.R., Ng, H.K., Royle, J.K., 1973. An oscillating bistable fluid amplifier for use as a flowmeter. *Fluidics Quarterly*, **5**(1):28-42.

Uzol, O., Camci, C., 1998. Oscillator Fin as a Novel Heat Transfer Augmentation Device for Gas Turbine Blade Cooling Applications. Proceedings of ASME Turbo Expo, Stockholm, Sweden.

Wang, H., Priestman, H., Beck, S.B.M., Boucher, R.F., 1996. Development of fluidic flowmeters for monitoring crude oil production. *Flow Measurement and Instrumentation*, **7**(2):91-98. [doi:10.1016/S0955-5986(97)00009-5]